MOLECULAR AND CELLULAR BIOLOGY, Nov. 2001, p. 7817–7825 Vol. 21, No. 22
0270-7306/01/$04.00+0 DOI: 10.1128/MCB.21.22.7817–7825.2001

Mice with a Targeted Deletion of the Tetranectin Gene Exhibit a Spinal Deformity

KOUSUKE IBA,[1]† MARIAN E. DURKIN,[1]‡ LISE JOHNSEN,[1]§ ERNST HUNZIKER,[2] KAREN DAMGAARD-PEDERSEN,[3] HONG ZHANG,[1] EVA ENGVALL,[4] REIDAR ALBRECHTSEN,[1] AND ULLA M. WEWER[1]*

The Institute of Molecular Pathology, University of Copenhagen,[1] and Department of Radiology, The Rigshospitalet University Hospital,[3] Copenhagen, Denmark; The M. E. Muller Institute for Biomechanics, University of Bern, Bern, Switzerland[2]; and The Burnham Institute, La Jolla, California[4]

Received 25 June 2001/Returned for modification 3 August 2001/Accepted 22 August 2001

Tetranectin is a plasminogen-binding, homotrimeric protein belonging to the C-type lectin family of proteins. Tetranectin has been suggested to play a role in tissue remodeling, due to its ability to stimulate plasminogen activation and its expression in developing tissues such as developing bone and muscle. To test the functional role of tetranectin directly, we have generated mice with a targeted disruption of the gene. We report that the tetranectin-deficient mice exhibit kyphosis, a type of spinal deformity characterized by an increased curvature of the thoracic spine. The kyphotic angles were measured on radiographs. In 6-month-old normal mice ($n = 27$), the thoracic angle was 73° ± 2°, while in tetranectin-deficient 6-month-old mice ($n = 35$), it was 93° ± 2° ($P < 0.0001$). In approximately one-third of the mutant mice, X-ray analysis revealed structural changes in the morphology of the vertebrae. Histological analysis of the spines of these mice revealed an apparently asymmetric development of the growth plate and of the intervertebral disks of the vertebrae. In the most advanced cases, the growth plates appeared disorganized and irregular, with the disk material protruding through the growth plate. Tetranectin-null mice had a normal peak bone mass density and were not more susceptible to ovariectomy-induced osteoporosis than were their littermates as determined by dual-emission X-ray absorptiometry scanning. These results demonstrate that tetranectin plays a role in tissue growth and remodeling. The tetranectin-deficient mouse is the first mouse model that resembles common human kyphotic disorders, which affect up to 8% of the population.

Tetranectin belongs to the family of C-type lectins and is composed of three identical, noncovalently linked 20-kDa subunits (for reviews, see references 27 and 49). Tetranectin binds to the fourth kringle domain of plasminogen and can stimulate plasminogen activation in vitro (14). Tetranectin also binds to calcium, fibrin, apolipoprotein A, and sulfated glycosaminoglycans. The mature tetranectin monomer of 181 amino acids consists of three functional domains encoded by separate exons (3, 22, 50). A short lysine-rich region at the N terminus binds to heparin (35). This domain is followed by an α-helical domain responsible for multimerization by forming a triple coiled-coil α-helix (39). The final 132 amino acids comprise a C-type lectin-like domain, homologous to the carbohydrate recognition domains of calcium-dependent animal lectins (18) and contain binding sites for calcium and plasminogen (23). The crystal structure of tetranectin is similar to that of mannose binding protein, a member of the collectin group of the C-type lectin superfamily, except that the presence of an extra disulfide bridge in tetranectin may restrict the flexibility of the C-type lectin-like domain (39). The human, mouse, and chicken tetranectin cDNA sequences and gene structures are very similar (3, 31, 44, 45, 50, 53).

Tetranectin is produced by many different cell types and is present in serum at a concentration of 10 mg/liter (32). During muscle cell development and regeneration, tetranectin expression marks active myogenesis in vivo and in vitro (52). Tetranectin is also expressed during bone development, and transfection studies suggest that tetranectin can induce osteogenesis (29, 51). The tetranectin concentration in serum decreases in pathological conditions such as cancer (26, 27) and myocardial infarction (33). While tetranectin cannot be detected by immunohistochemical methods in the extracellular matrix of normal adult tissues, it accumulates in the stroma of breast, ovarian, and colon carcinomas and colocalizes with plasminogen at the invasive front of melanomas (13, 17, 50). Because of the distinct binding properties of tetranectin and its dynamic expression in development and disease, one may expect that tetranectin plays a role in tissue remodeling. The precise function of tetranectin in these processes, however, is not known, and no human genetic disorders have yet been associated with mutations in the single-copy tetranectin gene located on chromosome 3p22-p21.3 (19).

In this study, we have evaluated the importance of tetranectin in development and disease. We demonstrate by generating mice with a targeted deletion that loss of tetranectin expression

* Corresponding author, Mailing address: Institute of Molecular Pathology, University of Copenhagen, Frederik V's vej 11, 2100 Copenhagen, Denmark. Phone: 45 35 32 60 56. Fax: 45 35 32 60 81. E-mail: ullaw@pai.ku.dk.

† Present address: Department of Orthopaedic Surgery, Monbetsu Hospital, Monbetsu, Japan.

‡ Present address: National Cancer Institute, National Institutes of Health, Bethesda, Md.

§ Present address: Department of Anatomy and Neurobiology, University of Southern Denmark, Odense, Denmark.

interferes with proper postnatal development of the vertebral bodies and results in a mild spine deformity.

MATERIALS AND METHODS

Generation of tetranectin-deficient mice. Mouse tetranectin genomic clones were isolated by screening a 129/SvJ library in lambda FIXII with the insert of the full-length mouse tetranectin cDNA clone pM-tna (31). The insert of one clone, λ15, was characterized by restriction enzyme mapping and sequencing and found to contain the entire mouse tetranectin gene, which spans 6.6 kb and consists of three exons (45). To construct the targeting vector, a 1.1-kb *Sac*I/*Stu*I fragment upstream of exon 1 and a 5.5-kb *Apa*I fragment containing exons 2 and 3 were inserted into pPNT (47), in the opposite orientation relative to the *neo*R gene. Integration of the vector by homologous recombination leads to deletion of a 1.3-kb fragment containing the first exon. The plasmid DNA was linearized with *Not*I and electroporated into CJ7 (129/SvImJ) embryonic stem (ES) cells. Cell culture, electroporation, and selection in G418 and ganciclovir were performed as described previously (25). ES clones surviving drug selection were screened for homologous recombination by Southern blotting as described below, and 11 out of 132 clones were found to have one copy of the correctly targeted tetranectin allele. Several clones positive for the mutated gene were microinjected into 3.5-day C57BL/6J blastocysts to generate chimeric animals. Chimeras derived from ES clones 90 and 29 showed germ line transmission of the disrupted tetranectin gene, and these were mated to C57BL/6J mice to generate animals heterozygous for the mutant allele. Heterozygous males and females were bred to produce homozygous mice. C57BL/6J mice were obtained from M&B A/S, Ry, Denmark, and 129/SvImJ mice were obtained from The Jackson Laboratory. The mice had free access to drinking water and a standard chow containing 0.9% calcium and 0.7% phosphorus (Altromin no. 1324; C. Petersen a/s, Ringsted, Denmark). The experiments were conducted according to the animal experimental guidelines of the Animal Inspectorate, Denmark.

Genotyping of ES cells and mice. Genomic DNA from ES cells and mouse tail biopsy specimens was digested with *Bgl*II, fractionated on 1% agarose gels, and blotted onto nylon membranes. The blots were hybridized to a genomic DNA probe upstream of the 5′ *Sac*I/*Stu*I fragment used to construct the targeting vector. The probe detects a 6.7-kb *Bgl*II fragment in the wild-type allele and a 3.2-kb fragment in the mutant allele.

RT-PCR and Northern blot analysis. RNA was isolated from various tissues and primary cell cultures using the TRIzol reagent (Gibco-BRL). Reverse transcription-PCR (RT-PCR) and Northern blotting were performed essentially as described previously (51, 52). For RT-PCR, cDNA was synthesized using the Moloney murine leukemia virus reverse transcriptase as recommended by the manufacturer (Stratagene). Aliquots of cDNA equivalent to 125 ng of total RNA were amplified with the forward primer 5′-GCAGTATGGGATTTTGGG (nucleotides [nt] 77 to 94 of GenBank sequence U08595) and the reverse primer 5′-GGCACTTCAAGTTCACCTTGGTG (complementary to nt 303 to 325). After an initial denaturation at 95°C for 40 s, 35 cycles of denaturation at 94°C for 40 s, annealing at 60°C for 40 s, and extension at 72°C for 60 s were carried out. As a control, the same cDNA samples were amplified using primers for the mouse glyceraldehyde-3-phosphate dehydrogenase cDNA sequence (GenBank M32599), namely, 5′-AAGGTCATCCCAGAGCTGAACG (nt 695 to 716) and 5′-TGTCATACCAGGAAATGAGC (complementary to nt 967 to 986), using the same conditions as above, except that the annealing temperature was 55°C. For Northern blots, 15 μg of total RNA per lane was separated on 1% agarose-formaldehyde gels and blotted onto Hybond N^+ nylon membranes (Amersham). Hybridization was carried out using the [α-^{32}P]dCTP-labeled mouse tetranectin cDNA probe and QuikHyb hybridization solution (Stratagene). After washing three times with 2× SSC (1× SSC is 0.15 M NaCl plus 0.015 M sodium citrate)–0.1% sodium dodecyl sulfate (SDS) at 65°C and twice with 0.2 × SSC–0.1% SDS at 65°C, the blots were exposed to Kodak X-Omat AR film at −80°C with intensifying screens.

Immunoblotting. Serum samples were boiled in SDS-polyacrylamide gel electrophoresis sample buffer, separated on 10 to 20% gradient gels together with See Blue molecular weight markers (Novex), and transferred to nitrocellulose BA85 paper (Schleicher and Schuell). Nitrocellulose strips were incubated in 0.05 M Tris-HCl (pH 7.4)–0.15 M NaCl–0.2% antifoam B for 15 min at room temperature. The strips were incubated with polyclonal antiserum (rb 107) to mouse tetranectin (52) diluted 1:200 in nonfat dry milk solution overnight at 4°C with gentle shaking, followed by a peroxidase-conjugated goat anti-rabbit immunoglobulin G secondary antibody. The blots were developed using the SuperSignal chemiluminescence kit from Pierce.

Radiography. Mice were anesthetized and examined in a lateral position using a Siemens Mammomat 3000 with exposure parameters of 25 mA and 27 kV. The X-ray images were documented by an Agfa analog to the digital converting system ADC70.8×10′ and stored in a PACS system. Examination of X-rays was performed on hard-copy films and on a soft-copy monitor. The Cobb method was used for measuring angles of kyphosis Th 7-L 4 (thoral vertebral body 7 to lumbal vertebral body 4) as previously described (7). The vertebral bodies of the thoracic and lumbar spine were analyzed with regard to size and configuration including the definition and margin of the terminal plates.

Ovariectomy and bone mass density (BMD) measurements by dual- emission X-ray absorptiometry (DEXA). Mice were anesthetized and either ovariectomized (OVX) or sham-operated on (SHAM). In vivo bone mass densitometry was performed by DEXA scanning using a PIXImus mouse densitometer (Lunar) with a resolution of 0.18 by 0.18 pixels, an image area of 80 by 65 mm, and an X-ray generator with a stationary anode of an 0.3-mm focal spot with a dual energy supply of 80-35 kV at 500 μA according to the instructions of the manufacturer. The intraindividual coefficient of variance (coefficient of variance = standard deviation/mean 100%) of BMD was calculated in four different groups each consisting of 14 to 20 mice and found to be in the range of 0.96 to 1.48%, which is similar to that obtained by Nagy and Clair (38). At least three consecutive scans were performed for each animal at each time point.

Histological analysis. Whole spines were fixed in formalin, dehydrated in ethanol, embedded in methylmethacrylate, and surface stained. The spines were then serially sectioned in the sagittal plane using a Leco diamond saw machine, and saw cuts (about 150 μm thick) were mounted on Plexiglas holders using Krazy glue. The saw cuts were then milled down by a Leica Polycut E microtome to a thickness of about 80 to 100 μm, polished, and surface stained using McNeil's tetrachrome, toluidine blue, and basic fuchsin.

Culture of primary muscle and osteoblast cells and muscle cells. Primary mouse osteoblast-like cells and muscle cells were isolated, cultured, and analyzed as described previously (30). Briefly, osteoblast-like cells were isolated from calvaria of newborn mice (0 to 3 days old) using 320 mg of collagenase (Sigma C5894) per liter and 0.25% trypsin (Gibco-BRL). Cells were grown in Dulbecco Modified Eagle Medium (DMEM) with 10% fetal bovine serum, and osteogenic capacity was tested by supplementing the medium with 50 μg of ascorbic acid (Sigma A2147) per ml and 10 mM β-glycerophosphate (Sigma G9891). Mineralization was observed after 10 to 14 days, and the cultures were stained with alizarin red S (Sigma A5533) after 21 days in culture. Primary muscle cell cultures were established from hindlimb muscles (0 to 3 days old) using a mixture of 0.15% trypsin and 0.1% dispase (both enzymes from Gibco-BRL). The cells were cultured with DMEM–20% fetal bovine serum and 2% chicken embryo extract (Gibco-BRL). After 3 to 4 days, the growth medium was replaced with differentiation medium containing DMEM–2% horse serum.

Growth curve and other analysis. Control (+/+) and tetranectin-deficient (−/−) female and male mice were weighed every week to monitor growth. Serum Ca^{2+}, alkaline phosphatase, and creatine kinase were measured. For statistical analysis, the Student *t* test was used and a *P* value of <0.05 was considered significant.

RESULTS

Generation of tetranectin-deficient mice. The strategy for disrupting the tetranectin gene is shown in Fig. 1A. Homologous recombination with the targeting vector results in deletion of the transcription start site and exon 1, which contains the translation start codon; such a deletion is predicted to abolish the synthesis of both tetranectin mRNA and protein. Two correctly targeted ES cell clones (90 and 29) were used to generate two strains of mice heterozygous for the mutated allele. Heterozygous animals were bred, and homozygous offspring were obtained at the expected frequency; thus, of 215 offspring of clone 90, the relative frequencies were 28% +/+, 48% +/−, and 24% −/−. Southern blot hybridization with three different probes confirmed the correct targeting of the tetranectin gene (Fig. 1B). To determine whether deletion of exon 1 resulted in loss of tetranectin mRNA expression, RT-PCR and Northern blot analysis were performed, and no tetranectin transcript was detected in several tissues from homozygous mice as well as in cultured cells derived from mice homozygous for the targeted allele (Fig. 2A to C). Tetranectin

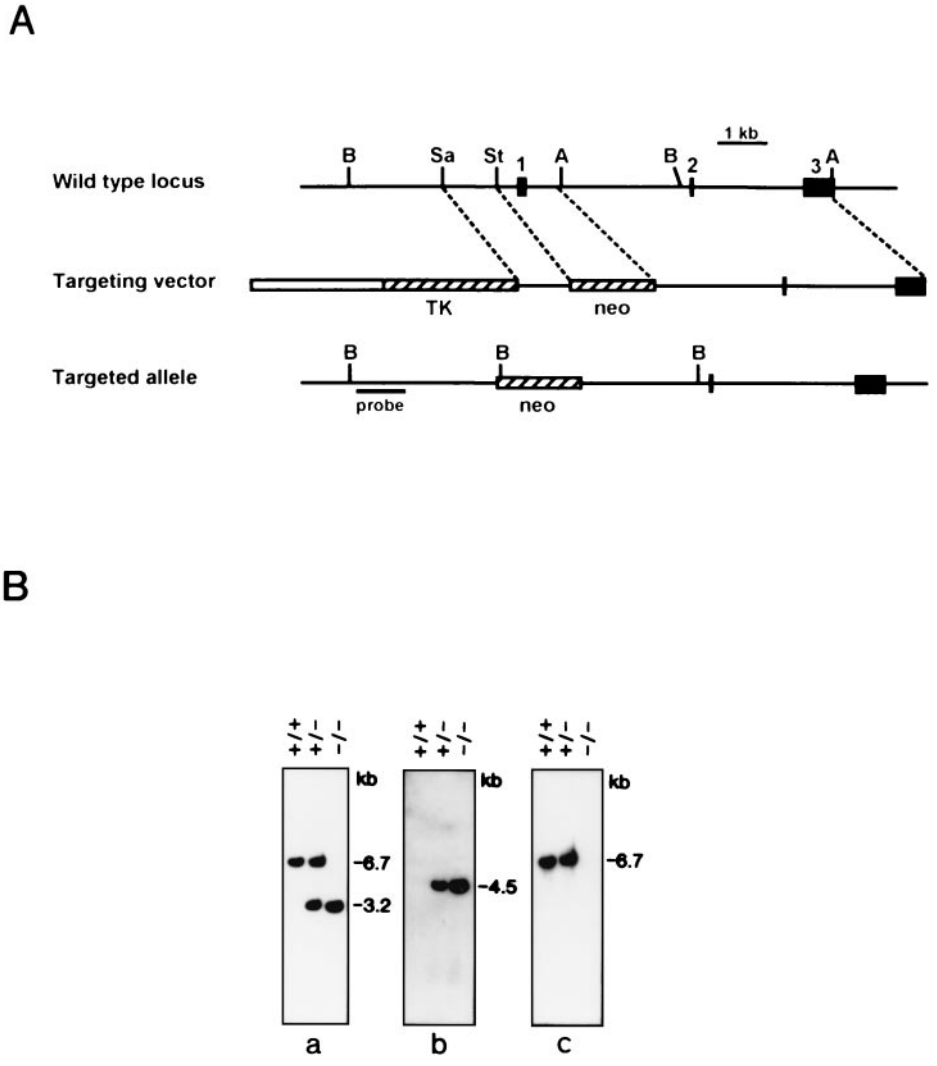

FIG. 1. Generation of mice with a targeted disruption of the tetranectin gene. (A) The restriction map and genomic structure of the wild-type mouse tetranectin gene are shown at the top. The three exons are numbered and represented by solid boxes. Restriction sites for *Bgl*II (B), *Sac*I (Sa), *Stu*I (St), and *Apa*I (A) are indicated. A diagram of the targeting vector is shown in the middle. The 1.1-kb *Sac*I/*Stu*I and 5.5-kb *Apa*I fragments were cloned into the pPNT vector. The thymidine kinase (TK) and neomycin-resistance (neo) cassettes of pPNT are represented by hatched boxes, and the plasmid backbone is depicted by an open box. The structure of the targeted allele is shown at the bottom. Homologous recombination between the targeting vector and the wild-type locus leads to deletion of the 1.3-kb *Stu*I/*Apa*I fragment containing exon 1 and insertion of the *neoR* cassette. The thick line indicates the 5′ external probe used for Southern blot screening of ES cells and mouse tail biopsy specimens. (B) Southern blot analysis of *Bgl*II-cut genomic DNA from normal mice (+/+) and from mice heterozygous (+/−) and homozygous (−/−) for the disrupted tetranectin allele. The blot was sequentially hybridized to the 5′ external probe (a), a fragment of the *neoR* gene (b), and a genomic probe containing exon 1 (c). In the correctly targeted allele, insertion of the *neoR* cassette will introduce an extra *Bgl*II site, and the 6.7-kb *Bgl*II band containing exon 1 will be replaced with bands of 3.2 and 4.5 kb carrying the tetranectin gene 5′-flanking DNA and the *neoR* gene, respectively.

is a serum protein that can readily be detected in wild-type mice by Western blotting (52). As shown in Fig. 2D, no tetranectin protein was detected in serum from mice homozygous for the disrupted gene. These results demonstrate that we have generated mice with a null allele of the tetranectin gene.

Tetranectin-deficient mice develop an increased curvature of the thoracic spine. The tetranectin-deficient mice appeared healthy, and no significant difference in growth rate was observed between control and tetranectin-deficient mice (Fig. 3). The tetranectin-deficient mice were fertile and lactated normally, and no apparent reduction in litter size was noted, indicating that neither fetal nor maternal tetranectin is required for normal embryonic development. Homozygous mice were successfully bred through three generations and had a similar life span as their littermate controls. All major organs were examined histologically, and no obvious pathological changes were observed (data not shown). Notably, we did not observe any apparent pathological changes in skeletal muscles. However, the tetranectin-deficient mice developed an abnormal anteroposterior curvature of the spine known as kyphosis, which became apparent at 3 to 6 months of age. The kyphosis appeared fixed, i.e., the deformity was unchanged as the mice moved. The kyphotic angles (Th 7-L 4) in 6-, 12-, and 18-month-old mice were measured on radiographs using the Cobb

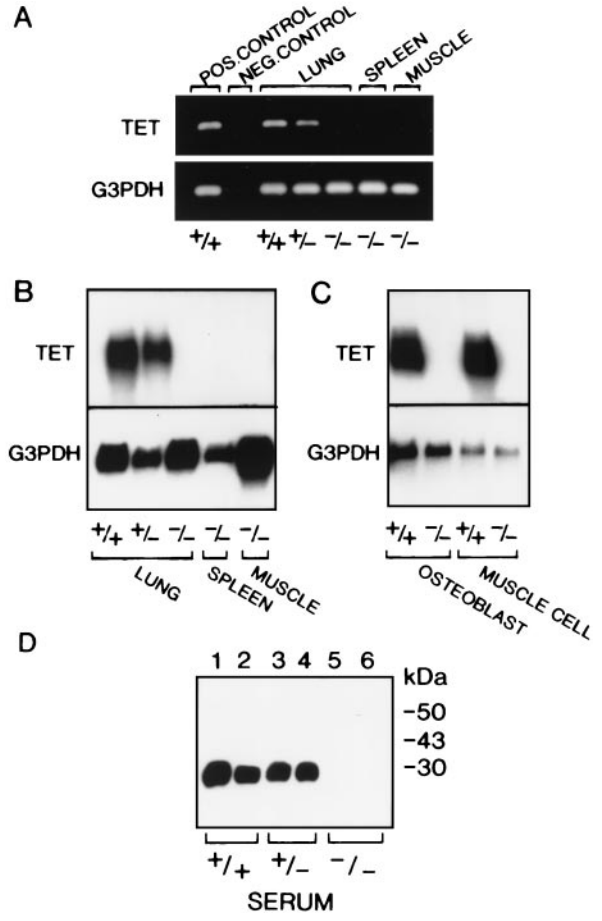

FIG. 2. Analysis of tetranectin gene expression in mice with a targeted tetranectin allele. (A) RT-PCR analysis of wild-type (+/+) and heterozygous (+/−) mouse lung tissue revealed a 249-bp tetranectin (TET) fragment, while no product was amplified from the lung, spleen, and muscle of homozygous (−/−) mice when RT-PCR was performed using TET-specific primers as described in Materials and Methods. A 292-bp fragment was amplified in all samples using mouse glyceraldehyde-3-phosphate dehydrogenase (G3PDH) primers. Normal mouse muscle tissue served as a positive control, and an RT reaction in which no reverse transcriptase enzyme was added served as a negative control. (B) Northern blot analysis of total RNA isolated from lung, spleen, and muscle tissue extracted from wild-type (+/+), heterozygous (+/−), and homozygous (−/−) mice. (C) Northern blot of total RNA isolated from primary osteoblasts or muscle cells established from wild-type (+/+) and homozygous (−/−) mice. The 1-kb tetranectin transcript is observed in tissues and cell cultures from wild-type (+/+) and heterozygous (+/−) mice but not in homozygous (−/−) samples. (D) Western blot analysis of duplicate samples revealed the 27-kDa TET monomer in serum from wild-type (+/+) and heterozygous (+/−) mice, but no TET protein was detected in samples derived from homozygous (−/−) mice using a polyclonal antiserum to mouse TET.

method (7) and compared to those of control mice (Fig. 4 and Table 1). Mice derived from both independent clones from both strains were analyzed (Table 1). A statistically significant difference was observed between tetranectin-deficient mice and control mice; in 6-month-old heterozygous mice derived from clone 90 ($n = 27$), the mean thoracic angle was 73°C ± 2°, while in tetranectin-deficient 6-month-old mice from the same clone ($n = 35$), it was 93° ± 2° ($P < 0.0001$). Tetranectin nulls also exhibited a cervical lordosis. Out of 60 tetranectin-deficient mice examined in more detail, 23 had radiological abnormalities of the vertebrae that were pathological and not seen in the control mice. The three major pathological changes of the vertebrae were anterior wedging, i.e., reduction of the anterior height of the corpora due to angulation of the terminal plates, with occasional lack of definition or irregularity of the terminal plates; rounding or a tip-like look of the vertebrae; and an overall shortening and/or broadening of the vertebrae. The intervertebral disk spaces of the tetranectin-deficient mice were of normal size and width. Scoliosis, which is characterized by an abnormal lateral curvature of the spine, was not observed in any of the tetranectin-deficient mice, nor were signs of halisteresis or compression fractures observed. No pathological changes of the long bones were observed by X-ray analysis. No difference in femoral bone length/weight ratios was found; at 6 months of age, the ratios were 0.53 ± 0.1 mm/g for control mice ($n = 19$) and 0.49 ± 0.07 mm/g for tetranectin-deficient mice ($n = 25$) ($P = 0.3$), and at 12 months of age, the ratios were 0.56 ± 0.06 mm/g for control mice ($n = 19$) and 0.59 ± 0.08 mm/g for tetranectin-deficient mice ($n = 15$) ($P = 0.8$). Levels of alkaline phosphatase, Ca^{2+}, and creatine kinase in serum revealed no pathological changes in the tetranectin-deficient mice (data not shown).

Tetranectin-null mice develop a normal peak BMD and are not more susceptible to ovariectomy-induced osteoporosis than are control mice. Since tetranectin can enhance bone formation (51), we hypothesized that, in tetranectin-deficient mice, the supportive cancellous bone of the vertebrae could be weakened due to impaired bone formation during the postnatal growth period. To test this hypothesis, we measured the subcranial total body BMD in 16-week-old mice by DEXA scanning using a PIXImus mouse densitometer, but no difference between tetranectin-deficient mice (54.3 ± 2.8 g/cm^2; $n = 29$) and control mice (52.0 ± 2.3 g/cm^2; $n = 14$) was observed (Table 2). We also investigated whether lack of tetranectin expression might reduce regeneration in the adult mice and

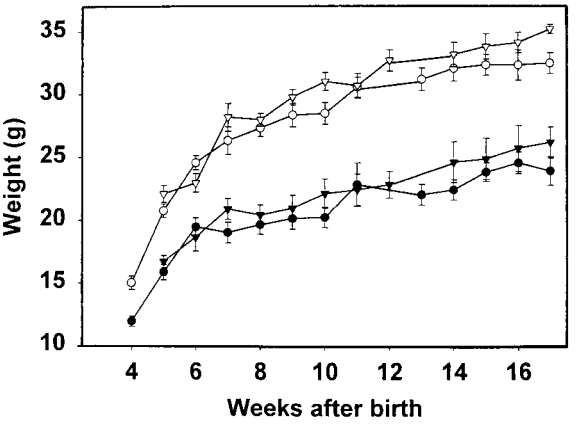

FIG. 3. Growth curves of tetranectin knockout mice. The weights of wild-type (+/+) and homozygous (−/−) female and male mice were recorded every week for 17 weeks. Wild-type females are indicated by inverted solid triangles, homozygous females are indicated by solid circles, wild-type males are indicated by open inverted triangles, and homozygous males are indicated by open circles. The slight difference in weight between wild-type and tetranectin-deficient mice is not statistically significant.

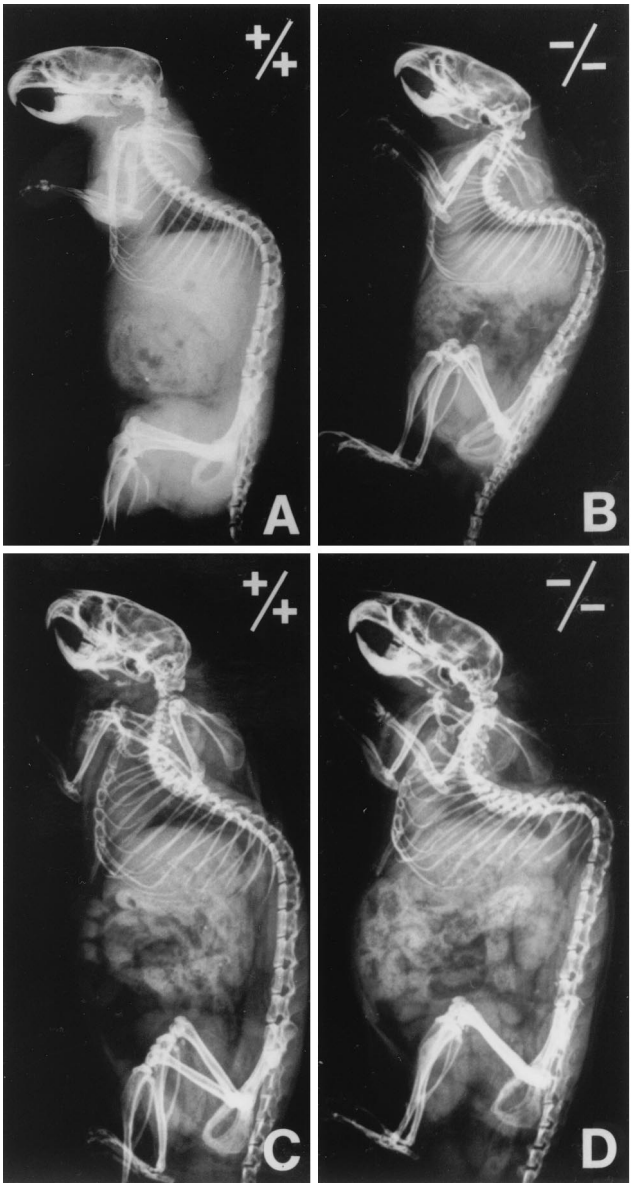

FIG. 4. X-ray analysis of the kyphotic spine of the tetranectin knockout mice. Radiographs of a wild-type (+/+) 6-month-old mouse (A), a homozygous (−/−) 6-month-old mouse (B), a wild-type (+/+) 12-month-old mouse (C), and a homozygous (−/−) 12-month-old mouse (D) are shown. Note the pronounced cervical lordosis and the thoracic kyphosis in tetranectin-null mice in panels B and D.

promote the development of osteoporosis, a situation in which normally mineralized bone mass decreases such that it no longer provides adequate mechanical support. Bone loss was induced by ovariectomy, a widely used experimental model system of postmenopausal osteoporosis (2, 16). Sixteen-week-old mice were ovariectomized or sham operated on, and the BMD was measured 3, 6, and 12 weeks after the operation. Twelve weeks following ovariectomy, the BMD values were reduced by 8.5% in the tetranectin-deficient mice, a reduction similar to that observed in control ovariectomized mice (9.4%) and in C57BL/6J (12%) and 129/SvImJ (8.7%) mice (Table 2). Finally, when primary osteoblast cultures were examined, no apparent difference with regard to onset or degree of mineralization was observed between tetranectin-deficient mice and control mice (data not shown). We conclude that the spinal abnormalities seen in tetranectin-deficient mice are not attributable to a defect in bone formation or mineralization.

TABLE 1. The thoracic kyphosis of the spine (Th 7-L 4) of the tetranectin-deficient mice and control mice[a]

Clone	Age (mo)	Angle (°)		*P*
		Control (Tet +/−)	Null (Tet −/−)	
90	6	73 ± 2 (n = 27)	93 ± 2 (n = 35)	<0.00001
	12	84 ± 3 (n = 8)	101 ± 2 (n = 15)	<0.0002
	18	77 ± 3 (n = 8)	101 ± 2 (n = 18)	<0.00001
29	6	76 ± 2 (n = 13)	98 ± 6 (n = 8)	<0.001

[a] Tet, tetranectin.

Histological analysis of the spine of tetranectin-deficient mice reveals variable changes. The morphological appearance of the spines of 10-day-, 14-day-, 6-month-, and 12-month-old tetranectin-deficient and control mice was investigated by methacrylate-based light microscopic analysis of formalin-fixed tissue (Fig. 5). No pathological changes were observed in 10-day- and 14-day-old tetranectin-deficient mice (data not shown). The 6- and 12-month-old tetranectin-deficient mice exhibited an increased spinal curvature associated with an asymmetric development of the intervertebral disk and an asymmetric activity of the growth plates. As can be seen in Fig. 5A to D, the posterior convex part of the intervertebral disks was loose in structure and the anterior concave part was compressed in tetranectin-deficient mice compared to the control mice. Moreover, in some tetranectin-deficient mice, the growth plates were more disorganized and narrow, were irregular in size compared to those of the control mice, and exhibited a higher degree of variation in cellular size and shape than that seen in normal tissue. At 12 months of age, irregular growth plates and disk protrusions were seen in tetranectin-deficient mice (Fig. 5E to H). The other parts of the vertebral bodies were normal in structure, size, and trabecular density as well as in bone marrow content. Together, those observations indicate that tetranectin deficiency leads to an apparent progressive

TABLE 2. Peak BMD and changes in BMD following ovariectomy

Mouse strain and group	n	Day of operation		12 wk after operation	
		Wt (g)	BMD_0 (mg/cm^2)	BMD_{12} (mg/cm^2)	Reduction (%)[a]
C57BL/6J	19	22.0 ± 1.3	46.3 ± 1.2		12.0
OVX	11	22.0 ± 1.0	45.9 ± 1.0	44.5 ± 1.8	
SHAM	8	21.9 ± 1.7	46.8 ± 1.1	50.1 ± 1.4	
129S3/SvImJ	20	21.4 ± 1.5	54.0 ± 2.3		8.7
OVX	10	21.7 ± 2.0	54.0 ± 3.0	52.1 ± 2.2	
SHAM	10	21.2 ± 0.9	53.9 ± 1.4	56.8 ± 1.6	
Null (Tet−/−)	29	24.9 ± 2.0	54.3 ± 2.8		8.5
OVX	14	24.7 ± 2.2	53.8 ± 2.9	51.6 ± 2.4	
SHAM	15	25.0 ± 1.7	54.7 ± 2.7	56.2 ± 2.9	
Control (+/+)	14	23.8 ± 1.7	52.0 ± 2.3		9.4
OVX	5	23.1 ± 1.2	51.3 ± 0.9	48.8 ± 2.0	
SHAM	5	24.0 ± 1.7	52.5 ± 2.5	53.7 ± 2.8	

[a] Calculated as reduction (%) = $(BMD_{12\ SHAM} - BMD_{12\ OVX})/BMD_0 \times 100$.

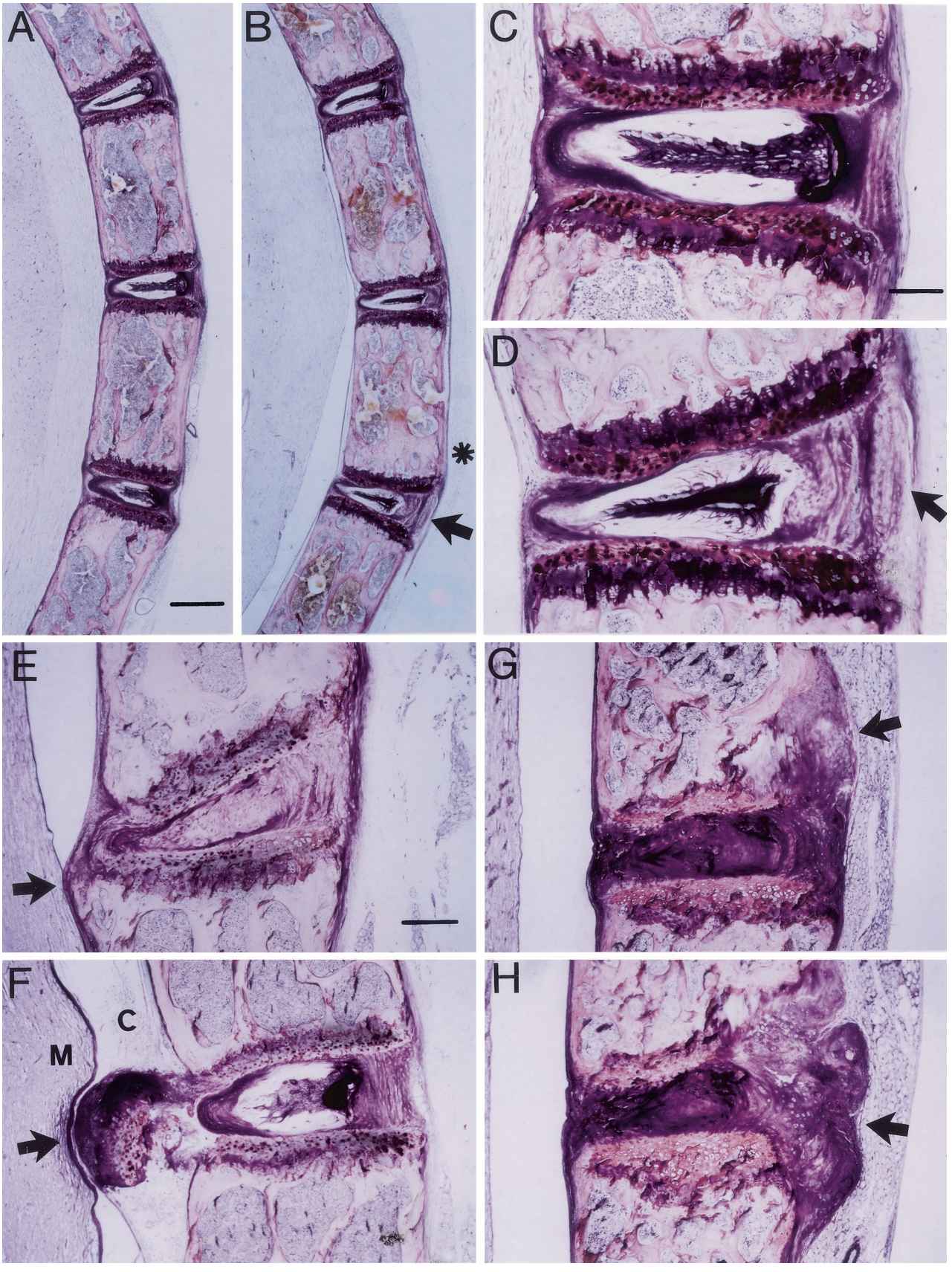

FIG. 5. Histological analysis of the tetranectin knockout mice. Sagittal sections of spines from control (+/+) and tetranectin-deficient (−/−) mice are shown. All sections are in the same orientation and as indicated in panel A. Control mice are demonstrated in panels A and C, and

weakening of the growth plate and that the rate of progression varies among the mice.

DISCUSSION

In the present study, we report that mice with targeted disruption of the gene encoding tetranectin, a protein present in serum and extracellular matrix, exhibit a kyphotic spine deformity and may serve as an animal model for some human kyphotic disorders such as Scheuermann's disease.

We have previously shown that tetranectin might be involved in muscle and bone cell differentiation and maturation (29, 51), prompting us to ask whether mice lacking tetranectin would manifest a musculoskeletal disorder. Although tetranectin-null mice were viable, bred normally, and had no apparent muscle pathology, they exhibited a kyphotic spine. This deformity was not apparent at birth but developed gradually until increased thoracic anteroposterior curvature was apparent at 6 months of age. Radiological and histological examination of the vertebrae did not reveal consistently severe structural changes. A third of the tetranectin-deficient mice displayed an altered vertebral morphology by X-ray analysis. A consistent feature revealed by histological examination was an asymmetric development of the intervertebral disks and an asymmetric activity of the growth plates. Irregularities of the growth plate and protrusions of disk material were also observed. Since we did not observe any pathological changes of the musculature, these findings indicate that tetranectin is required for stabilizing the spine and that loss of tetranectin leads to a softening of the extracellular matrix of the bone and the intervertebral disks. How tetranectin deficiency leads to these changes at a molecular level remains to be determined. Proteolytic activity is essential for bone formation, and skeletal defects have been observed in mice deficient in matrix metalloproteinase-9/gelatinase B (48) and in membrane type I-matrix metalloproteinase (28). As tetranectin may activate plasminogen, it may be involved in the proteolysis of collagen, proteoglycans, or other extracellular matrix proteins that is necessary for remodeling of skeletal tissue. Alternatively, tetranectin could regulate the activity of osteogenic growth factors, either by proteolytic processing to the active form or by release from the extracellular matrix. The phenotype of the tetranectin-deficient mice is different from that of mice with a targeted inactivation of the plasminogen gene. The plasminogen-deficient mice are normal in appearance but suffer morbidity due to thrombosis (12); this may suggest that plasminogen activation is not involved in the effect of tetranectin on spinal development.

In humans, the most frequent cause of kyphosis in adolescence is Scheuermann's disease, also known as juvenile kyphosis or spinal osteochondrosis (1, 6, 10). It was first described in 1921 by Scheuermann (42) and later redefined in particular by Sørensen (46) and Bradford (6, 8, 10). It arises during childhood or adolescence and is reported to affect up to 8% of the population (discussed in reference 41). The clinical manifestations of kyphosis vary; in most cases, few symptoms are present, and it is often neglected and attributed to poor posture. In other cases, patients complain of fatigue and chronic back pain that becomes worse upon physical stress. Radiographically, Scheuermann's disease (41) and to some extent the tetranectin-deficient mice described here are characterized by wedge-shaped deformities of the vertebrae, growth plate irregularities, and narrowing of disk spaces. In some families, Scheuermann's disease shows an autosomal dominant form of inheritance (21, 24, 34, 36, 40). Scheuermann's disease has been suggested to be a disorder in collagen biosynthesis, although linkage to COL1A2 has been excluded (36). It will be interesting to determine whether Scheuermann's disease may in fact represent several distinct genetic entities, one of which may be due to a mutation in the tetranectin gene.

Kyphosis represents a manifestation of osteoporosis in the spine in older women. Osteoporosis is a severe and common disease; it is estimated that a Caucasian woman at age 50 has about 30% probability of experiencing at least one vertebral fracture during her remaining lifetime (15, 20). Moreover, it has been suggested that Scheuermann's disease could be a mild form of juvenile osteoporosis (9). These considerations led us to investigate the peak BMD of the tetranectin-deficient mice. However, we did not observe any association between the development of kyphosis and a decrease in BMD in the tetranectin-deficient mice, nor were the tetranectin-deficient mice more prone to developing osteoporosis after ovariectomy. This result demonstrates that tetranectin deficiency does not lead to a defect in mineralization and suggests that tetranectin plays other important roles in maintaining the integrity of the extracellular matrix of the spine.

Spinal deformitites characterized by kyphosis and kyphoscoliosis represent a clinical feature of a number of neuromuscular disorders of childhood, particularly congenital muscular dystrophy with rigid spine (RSMD-1) (37) and the X-linked Emery-Dreifuss muscular dystrophy (5). Likewise, several types of muscle disease in mice are associated with the development of a spinal deformity. For example, the *ky* (kyphoscoliosis) mutant suffers an autosomal recessive degenerative muscle disease with severe kyphoscoliosis (4, 11, 43). Notably, these forms of spinal deformities are secondary to the muscle disease and thus are different from the tetranectin-deficient mice, which exhibit no muscle pathology. We conclude that loss of tetranectin leads to a primary kyphotic spine deformity that becomes apparent during the postnatal growth phase. Our studies also strongly suggest that the primary defect occurs in the vertebral bone, where tetranectin is normally expressed, rather than in the cartilage, where tetranectin is normally not present (51).

In conclusion, we have generated mice with a targeted de-

tetranectin-deficient mice are shown in panels B and D to H. Note that the increased thoracic curvature in the tetranectin-deficient mice is associated with a thickening and broadening of the vertebral bodies (asterisk in panel B). In the tetranectin-deficient mice, intervertebral disk material is asymmetrical in shape: expanded and loose in structure at the convex side (arrows in panels B and D) and narrowed and compressed at the concave side. Panels E to H demonstrate various degrees of irregular growth plates associated with protrusions of vertebral disk material into the cavum subarachnoidale (E and F) or into the vertebral bodies (G and H) (arrows). Mice shown in panels A to D are 6 months old, and those in panels E to H are 12 months old. M, medulla spinalis; C, cavum subarachnoidale. Bars, 300 (A and B), 85 (C and D), and 115 (E to H) μm.

letion of tetranectin and found that these mice exhibit a kyphotic spine abnormality that shares similarity with common kyphotic disorders in the human, such as Scheuermann's disease. It will now be feasible to screen for mutations in tetranectin in these patients. However, even in the absence of a primary gene defect in tetranectin in humans, the tetranectin-deficient mouse model should be valuable for researchers studying the pathogenesis and treatment of kyphotic disorders in humans.

ACKNOWLEDGMENTS

The study was supported by the Danish Medical Research Council; the Neye, Velux, and Haensch Foundations; by an EU grant, Quality of Life and Management of Living Resources (contract no. QLG1-CT-1999-00870, designated Genetic Resolution of Myopathies: European cluster [Myocluster]); and by The Scandinavia-Japan Sasakawa Foundation (Tokyo, Japan).

Brit Valentin is thanked for her skillful technical assistance. We thank Marian Young for advice on constructing the targeting vector and Reinhard Fässler and Thomas Voit for insightful discussions.

REFERENCES

1. **Aufdermaur, M., and M. Spycher.** 1986. Pathogenesis of osteochondrosis juvenilis Scheuermann. J. Orthop. Res. **4:**452–457.
2. **Bellino, F. L.** 2000. Nonprimate animal models of menopause: workshop report. Menopause **7:**14–24.
3. **Berglund, L., and T. E. Petersen.** 1992. The gene structure of tetranectin, a plasminogen binding protein. FEBS Lett. **309:**15–19.
4. **Blanco, G., G. R. Coulton, A. Biggin, C. Grainge, J. Moss, M. Barrett, A. Berquin, G. Maréchal, M. Skynner, P. van Mier, A. Nikitopoulou, M. Kraus, C. P. Ponting, R. M. Mason, and S. D. M. Brown.** 2001 The kyphoscoliosis (ky) mouse is deficient in hypertrophic responses and is caused by a mutation in a novel muscle-specific protein. Hum. Mol. Genet. **10:**9–16.
5. **Bonne, G., E. Mercuri, A. Muchir, A. Urtizberea, H. M. Becane, D. Recan, L. Merlini, M. Wehnert, R. Boor, U. Reuner, M. Vorgerd, E. M. Wicklein, B. Eymard, D. Duboc, I. Penisson-Besnier, J. M. Cuisset, X. Ferrer, I. Desguerre, D. Lacombe, K. Bushby, C. Pollitt, D. Toniolo, M. Fardeau, K. Schwartz, and F. Muntoni.** 2000. Clinical and molecular genetic spectrum of autosomal dominant Emery-Dreifuss muscular dystrophy due to mutations of the lamin A/C gene. Ann. Neurol. **48:**170–180.
6. **Bradford, D. S., J. H. Moe, and R. B. Winter.** 1973. Kyphosis and postural roundback deformity in children and adolescents. Minn. Med. **56:**114–120.
7. **Bradford, D. S., J. H. Moe, F. J. Montalvo, and R. B. Winter.** 1974. Scheuermann's kyphosis and roundback deformity. Results of Milwaukee brace treatment. J. Bone Jt. Surg. Am. Vol. **56:**740–758.
8. **Bradford, D. S., and J. H. Moe.** 1975. Scheuermann's juvenile kyphosis. A histologic study. Clin. Orthop. **110:**45–53.
9. **Bradford, D. S., D. M. Brown, J. H. Moe, R. B. Winter, and J. Jowsey.** 1976. Scheuermann's kyphosis: a form of osteoporosis? Clin. Orthop. **118:**10–15.
10. **Bradford, D. S.** 1981. Vertebral osteochondrosis (Scheuermann's kyphosis). Clin. Orthop. **158:**83–90.
11. **Bridges, L. R., G. R. Coulton, G. Howard, J. Moss, and R. M. Mason.** 1992. The neuromuscular basis of hereditary kyphoscoliosis in the mouse. Muscle Nerve **15:**172–179.
12. **Bugge, T. H., M. J. Flick, C. C. Daugherty, and J. L. Degen.** 1995. Plasminogen deficiency causes severe thrombosis but is compatible with development and reproduction. Genes Dev. **9:**794–807.
13. **Christensen, L., and I. Clemmensen.** 1991. Differences in tetranectin immunoreactivity between benign and malignant breast tissue. Histochemistry **95:**427–433.
14. **Clemmensen, I., L. C. Petersen, and C. Kluft.** 1986. Purification and characterization of a novel, oligomeric, plasminogen kringle 4 binding protein from human plasma: tetranectin. Eur. J. Biochem. **156:**327–333.
15. **Cummings, S. R., D. M. Black, and S. M. Rubin.** 1989. Lifetime risks of hip, Colles', or vertebral fracture and coronary heart disease among white postmenopausal women. Arch. Intern. Med. **149:**2445–2448.
16. **Delany, A. M., M. Amling, M. Priemel, C. Howe, R. Baron, and E. Canalis.** 2000. Osteopenia and decreased bone formation in osteonectin-deficient mice. J. Clin. Investig. **105:**1325.
17. **De Vries, T. J., P. E. De Wit, I. Clemmensen, H. W. Verspaget, U. H. Weidle, E. B. Brocker, D. J. Ruiter, and G. N. Van Muijen.** 1996. Tetranectin and plasmin/plasminogen are similarly distributed at the invasive front of cutaneous melanoma lesions. J. Pathol. **179:**260–265.
18. **Drickamer, K.** 1999. C-type lectin-like domains. Curr. Opin. Struct. Biol. **9:**585–590.
19. **Durkin, M. E., S. L. Naylor, R. Albrechtsen, and U. M. Wewer.** 1997. Assignment of the gene for human tetranectin (TNA) to chromosome 3p22→p21.3 by somatic cell hybrid mapping. Cytogenet. Cell Genet. **76:**39–40.
20. **Ensrud, K. E., D. M. Black, F. Harris, B. Ettinger, and S. R. Cummings.** 1997. Correlates of kyphosis in older women. The Fracture Intervention Trial Research Group. J. Am. Geriatr. Soc. **45:**682–687.
21. **Findlay, A., A. N. Conner, and J. M. Connor.** 1989. Dominant inheritance of Scheuermann's juvenile kyphosis. J. Med. Genet. **26:**400–403.
22. **Fuhlendorff, J., I. Clemmensen, and S. Magnusson.** 1987. Primary structure of tetranectin, a plasminogen kringle 4 binding plasma protein: homology with asialoglycoprotein receptors and cartilage proteoglycan core protein. Biochemistry **26:**6757–6764.
23. **Graversen, J. H., R. H. Lorentsen, C. Jacobsen, S. K. Moestrup, B. W. Sigurskjold, H. C. Thøgersen, and M. Etzerodt.** 1998. The plasminogen binding site of the C-type lectin tetranectin is located in the carbohydrate recognition domain, and binding is sensitive to both calcium and lysine. J. Biol. Chem. **273:**29241–29246.
24. **Halal, F., R. B. Gledhill, and C. Fraser.** 1978. Dominant inheritance of Scheuermann's juvenile kyphosis. Am. J. Dis. Child. **132:**1105–1107.
25. **Hogan, B., R. Beddington, F. Costantini, and E. Lacy.** 1994. Manipulating the mouse embryo: a laboratory manual. Cold Spring Harbor Laboratory Press, Plainview, N.Y.
26. **Høgdall, C. K., L. Christensen, and I. Clemmensen.** 1993. The prognostic value of tetranectin immunoreactivity and plasma tetranectin in patients with ovarian cancer. Cancer **72:**2415–2422.
27. **Høgdall, C. K.** 1998. Human tetranectin: methodological and clinical studies. APMIS Suppl. **86:**1–31.
28. **Holmbeck, K., P. Bianco, J. Caterina, S. Yamada, M. Kromer, S. A. Kuznetsov, M. Mankani, P. G. Robey, A. R. Poole, I. Pidoux, J. M. Ward, and H. Birkedal-Hansen.** 1999. MT1-MMP-deficient mice develop dwarfism, osteopenia, arthritis, and connective tissue disease due to inadequate collagen turnover. Cell **99:**81–92.
29. **Iba, K., N. Sawada, H. Chiba, U. M. Wewer, S. Ishii, and M. Mori.** 1995. Transforming growth factor-beta 1 downregulates dexamethasone-induced tetranectin gene expression during the *in vitro* mineralization of the human osteoblastic cell line SV-HFO. FEBS Lett. **373:**1–4.
30. **Iba, K., R. Albrechtsen, B. Gilpin, C. Frohlich, F. Loechel, A. Zolkiewska, K. Ishiguro, T. Kojima, W. Liu, J. K. Langford, R. D. Sanderson, C. Brakebusch, R. Fassler, and U. M. Wewer.** 2000. The cysteine-rich domain of human ADAM 12 supports cell adhesion through syndecans and triggers signaling events that lead to beta1 integrin-dependent cell spreading. J. Cell Biol. **149:**1143–1156.
31. **Ibaraki, K., C. A. Kozak, U. M. Wewer, R. Albrechtsen, and M. F. Young.** 1995. Mouse tetranectin: cDNA sequence, tissue-specific expression, and chromosomal mapping. Mamm. Genome **6:**693–696.
32. **Jensen, B. A., and I. Clemmensen.** 1988. Plasma tetranectin is reduced in cancer and related to metastasia. Cancer **62:**869–872.
33. **Kamper, E. F., L. Kopeikina, A. Mantas, C. Stefanadis, P. Toutouzas, and J. Stavridis.** 1998. Tetranectin levels in patients with acute myocardial infarction and their alterations during thrombolytic treatment. Ann. Clin. Biochem. **35:**400–407.
34. **Kewalramani, L. S., R. S. Riggins, and W. M. Fowler, Jr.** 1976. Scheuermann's kyphoscoliosis associated with Charcot-Marie-Tooth syndrome. Arch. Phys. Med. Rehabil. **57:**391–397.
35. **Lorentsen, R. H., J. H. Graversen, N. R. Caterer, H. C. Thøgersen, and M. Etzerodt.** 2000. The heparin-binding site in tetranectin is located in the N-terminal region and binding does not involve the carbohydrate recognition domain. Biochem. J. **347:**83–87.
36. **McKenzie, L., and D. Sillence.** 1992. Familial Scheuermann disease: a genetic and linkage study. J. Med. Genet. **29:**41–45.
37. **Moghadaszadeh, B., I. Desguerre, H. Topaloglu, F. Muntoni, S. Pavek, C. Sewry, M. Mayer, M. Fardeau, F. M. Tome, and P. Guicheney.** 1998. Identification of a new locus for a peculiar form of congenital muscular dystrophy with early rigidity of the spine, on chromosome 1p35–36. Am. J. Hum. Genet. **62:**1439–1445.
38. **Nagy, T. R., and A. L. Clair.** 2000. Precision and accuracy of dual-energy X-ray absorptiometry for determining *in vivo* body composition of mice. Obesity Res. **8:**392–398.
39. **Nielsen, B. B., J. S. Kastrup, H. Rasmussen, T. L. Holtet, J. H. Graversen, M. Etzerodt, H. C. Thøgersen, and I. K. Larsen.** 1997. Crystal structure of tetranectin, a trimeric plasminogen-binding protein with an alpha-helical coiled coil. FEBS Lett. **412:**388–396.
40. **Nielsen, O. G., and P. Pilgaard.** 1987. Two hereditary spinal diseases producing kyphosis during adolescence. Acta Paediatr. Scand. **76:**133–136.
41. **Resnick, D., and G. Niwayama.** 1988. Diagnosis of bone and joint disorders, 2nd ed., Vol. 5, p. 3320–3326. The W. B. Saunders Co. Philadelphia, Pa.
42. **Scheuermann, H.** 1990. Kyphosis dorsalis juvenilis. Ugeskr. Læg. **82:**385–393.
43. **Skynner, M. J., U. Gangadharan, G. R. Coulton, R. M. Mason, A. Nikitopoulou, S. D. Brown, and G. Blanco.** 1995. Genetic mapping of the mouse neuromuscular mutation kyphoscoliosis. Genomics **25:**207–213.
44. **Sørensen, C. B., L. Berglund, and T. E. Petersen.** 1995. Cloning of a cDNA encoding murine tetranectin. Gene **152:**243–245.

45. **Sørensen, C. B., L. Berglund, and T. E. Petersen.** 1997. Cloning of the murine tetranectin gene and 5′-flanking region. Gene **201:**199–202.
46. **Sørensen, K. H.** 1964. Scheuermann's juvenile kyphosis. Munksgaard, Copenhagen, Denmark.
47. **Tybulewicz, V. L., C. E. Crawford, P. K. Jackson, R. T. Bronson, and R. C. Mulligan.** 1991. Neonatal lethality and lymphopenia in mice with a homozygous disruption of the c-abl proto-oncogene. Cell **65:**1153–1163.
48. **Vu, T. H., J. M. Shipley, G. Bergers, J. E. Berger, J. A. Helms, D. Hanahan, S. D. Shapiro, R. M. Senior, and Z. Werb.** 1998. MMP-9/gelatinase B is a key regulator of growth plate angiogenesis and apoptosis of hypertrophic chondrocytes. Cell **93:**411–422.
49. **Wewer, U. M., and R. Albrechtsen.** Tetranectin. *In* The encyclopedia of molecular medicine, in press.
50. **Wewer, U. M., and R. Albrechtsen.** 1992. Tetranectin, a plasminogen kringle 4-binding protein. Cloning and gene expression pattern in human colon cancer. Lab. Investig. **67:**253–262.
51. **Wewer, U. M., K. Ibaraki, P. Schjørring, M. E. Durkin, M. F. Young, and R. Albrechtsen.** 1994. A potential role for tetranectin in mineralization during osteogenesis. J. Cell. Biol. **127:**1767–1775.
52. **Wewer, U. M., K. Iba, M. E. Durkin, F. C. Nielsen, F. Loechel, B. J. Gilpin, W. Kuang, E. Engvall, and R. Albrechtsen.** 1998. Tetranectin is a novel marker for myogenesis during embryonic development, muscle regeneration, and muscle cell differentiation *in vitro*. Dev. Biol. **200:**247–259.
53. **Xu, X., B. Gilpin, K. Iba, A. Maier, E. Engvall, R. Albrechtsen, and U. M. Wewer.** 2001. Tetranectin in slow intra- and extrafusal chicken muscle fibers. J. Muscle Res. Cell Motil. **22:**121–132.